Materials Transactions, Vol. 60, No. 9 (2019) pp. 2059 to 2068

Direct Deoxidation of Ti by Mg in $MgCl_2$–$HoCl_3$ Flux

Lingxin Kong, Takanari Ouchi* and Toru H. Okabe

Institute of Industrial Science, The University of Tokyo, Tokyo 153-8505, Japan

A new method for removing the dissolved oxygen (O) in titanium (Ti) is developed, wherein magnesium chloride–holmium chloride ($MgCl_2$–$HoCl_3$) and Mg are used as a flux and a reducing agent, respectively. Through the thermodynamic assessment using a p_{O_2}–p_{Cl_2} diagram as well as the experimental results, the deoxidation of Ti to a level below 1000 mass ppm O (and even 500 mass ppm O) via the formation reaction of holmium oxychloride (HoOCl), O (in Ti) + Mg + $HoCl_3$ → HoOCl + $MgCl_2$, was confirmed. The deoxidation limit decreases with the increase of the activity of $HoCl_3$ in the $MgCl_2$–$HoCl_3$ flux. One advantage of this method is that the activity of the deoxidized product, a_{MgO}, in the system can be effectively maintained at a low level by the formation of HoOCl. The E–pO^{2-} diagram of the M–O–Cl system (M = Ho, Mg) constructed in this study indicates that the electrochemical deoxidation of Ti scraps in $MgCl_2$–$HoCl_3$ system will be more effective because the a_{MgO} can be further decreased via the formation of HoOCl, and/or the electrochemical oxidation of oxide ions on the carbon anode. This new deoxidation technique using rare-earth-containing $MgCl_2$ flux can be applied to the recycling of Ti scraps in the future. [doi:10.2320/matertrans.MT-M2019135]

(Received May 9, 2019; Accepted June 24, 2019; Published August 25, 2019)

Keywords: *deoxidation, Ti, rare earth metals, magnesium chloride, HoOCl, electrochemical deoxidation, recycling*

1. Introduction

Titanium (Ti) and its alloys are well known for their high specific strength, lightness, and corrosion resistance.[1)] However, unlike common metals (e.g., steel, aluminum, zinc, tin), Ti is only applied in a few areas such as aerospace, bio-medical, and sports[2)] because of the high production cost of metallic Ti from its ores, despite the fact that Ti is the ninth most abundant element in the earth's crust with a reserve of 0.7%.[3)]

At present, Ti is mainly produced by the Kroll process,[4)] in which titanium tetrachloride ($TiCl_4$) is reduced by Mg in a reaction retort made of steel at 1073–1273 K. Ti sponge (virgin metal) obtained in the reduction process is subsequently melted to form an ingot, which is used to fabricate wrought Ti products. Although the Kroll process has the advantage of producing Ti with low-O content, the production cost is very high owing to the long processing time and high facility requirements. In addition, Ti scraps of greater weight than Ti products themselves are usually generated during the production of Ti products. Furthermore, increasing demand for Ti, particularly in the aerospace industry, has led to a growth in the amount of Ti scrap waste from the fabrication of Ti products.[5)] The recycling of Ti scraps, therefore, it has become imperative for Ti industries to solve the contradiction between the high production cost of Ti and the increased amount of waste Ti.

The O is the main harmful impurity in Ti and has a strong influence on the performance of Ti.[6)] The O content in Ti usually increases during the melting, casting, and machining processes because of the strong affinity of Ti for O at high temperatures.[5,7,8)] The O content of Ti products is usually higher than that of Ti sponge, which will be further increased during service processes, especially when Ti products are exposed to air at elevated temperatures. Therefore, Ti scraps often contain O concentrations ranging between 2000 and 4000 mass ppm O, which is significantly higher than that in the virgin metals for producing ingots.[7,9)] Currently, the Ti scrap with a high O concentration is usually used as an additive in steel production instead of being recycled.

The most effective way to recycle the Ti scrap is to directly re-melt it with the Ti sponge. However, O dissolved in the Ti scrap cannot be removed during conventional re-melting processes. Effective, nonpolluting, and economical processes for removing O directly from Ti scraps are therefore highly desirable.

Many techniques have been proposed and examined for the direct removal of O from Ti. Figure 1 summarizes the features of some representative deoxidation techniques,[9–11)] including the deoxidation technique employed in this study. For example, solid-state electrotransport (SSE)[12)] is an effective method for removing O from Ti. However, this method has considerable limitations in terms of the initial O content and the geometry of sample, and is applicable only to the treatment of a small amount of waste.[13)]

As shown in Fig. 1(b), direct deoxidation of Ti using reactive metals (e.g. Ca, Y, and Ho) as deoxidants is also possible. As shown in Table 1,[5,9,14,15)] Ca, Y, and Ho are candidates for use as deoxidants. For example, at 1173 K, the calculated deoxidation limit of Ca/CaO equilibrium is 320 mass ppm O, and that of Y/Y_2O_3 and Ho/Ho_2O_3 equilibrium are 130 mass ppm O and 260 mass ppm O, respectively. Since metallic Ca has a strong affinity for O and is relatively low cost, deoxidation using Ca/CaO equilibrium has been mainly employed from the early stage of development.[16–29)] The deoxidation limit of Ca/CaO equilibrium ($a_{CaO} = 1$) under most conditions is less than 500 mass ppm O. Compared with Ca, Y and Ho, the deoxidation capacity of Mg is low due to the weak affinity of Mg for O. For example, at 1300 K, the calculated value of the deoxidation limit of Mg/MgO equilibrium is 25000 mass ppm O, and the experimental value is 12100 mass ppm O,[5)] which is much higher than that of Ca/CaO equilibrium. In order to remelt the Ti scraps with the virgin metals for producing Ti ingots, the O concentration in Ti should be reduced to the level of Ti sponge (approximately 500 mass ppm O).

In addition to the affinity, the deoxidation limit of M/MO_x equilibrium also depends on the activity of the deoxidation

*Corresponding author, E-mail: t-ouchi@iis.u-tokyo.ac.jp

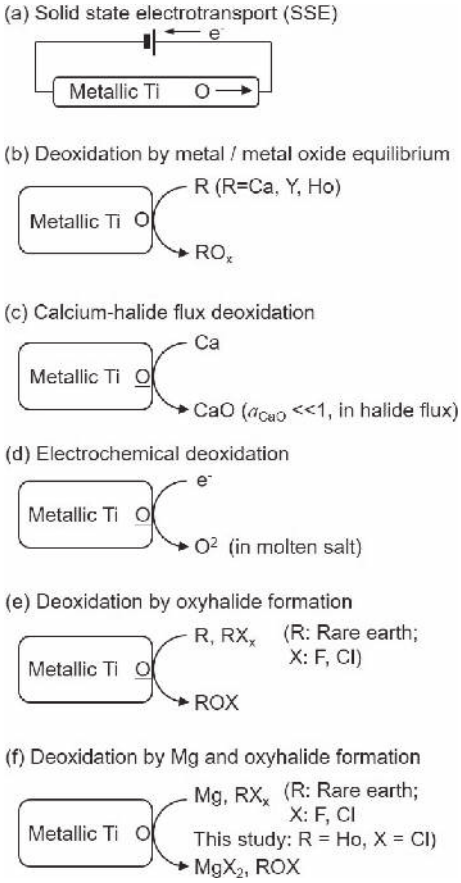

Fig. 1 Principles of representative purification methods that are capable of reducing the O content in solid Ti to 500 mass ppm O or less.[9)]

Table 1 Calculated partial pressure of O_2 and the theoretical O level in β-Ti under various equilibrium conditions at 1173 K.[5,9,14,15)]

	O_2 partial pressure at 1173 K, p_{O_2} / atm	Theoretical O conc. in β-Ti at 1173 K, C_O (mass ppm)
Mg/MgO eq.	8.0×10^{-43}	19300[a]
Ca/CaO eq.	2.2×10^{-46}	320
Y/Y_2O_3 eq.	3.3×10^{-47}	130
Ho/Ho_2O_3 eq.	1.4×10^{-46}	260
Nd/Nd_2O_3 eq.	1.3×10^{-44}	2500[a]
Pr/Pr_2O_3 eq.	1.9×10^{-44}	3000[a]
Ce/Ce_2O_3 eq.	3.1×10^{-44}	3800[a]
La/La_2O_3 eq.	4.6×10^{-44}	4700[a]
$Y/YOCl/YCl_3$ eq.	1.1×10^{-51}	< 1
$Ho/HoOCl/HoCl_3$ eq.	1.9×10^{-49}	9
$Pr/PrOCl/PrCl_3$ eq.	7.5×10^{-49}	20
$La/LaOCl/LaCl_3$ eq.	2.4×10^{-48}	30
$Ce/CeOCl/CeCl_3$ eq.	8.0×10^{-48}	60
$Nd/NdOCl/NdCl_3$ eq.	9.6×10^{-48}	70
Ca/(CaO) ($a_{CaO} = 0.031$) eq.	2.1×10^{-49}	10
Mg/(MgO)[b] ($a_{MgO} = 0.026$) eq.	5.3×10^{-46}	500
$Mg/MgCl_2/YOCl/YCl_3$ eq.	3.0×10^{-49}	10[c]
$Mg/MgCl_2/HoOCl/HoCl_3$ eq.	1.4×10^{-47}	80[d]

a: Larger than the solubility of O in β-Ti (ca. 2200 mass ppm O) at 1173 K.
b: The a_{MgO} in Mg/MgO eq. should be lowered to 0.026 to produce Ti with 500 mass ppm O.
c: The calculated deoxidation equilibrium ($Mg/MgCl_2/YOCl/YCl_3$ eq., $a_i = 1$).
d: The calculated deoxidation equilibrium ($Mg/MgCl_2/HoOCl/HoCl_3$ eq., $a_i = 1$).

Table 2 Solubility of oxide (MO_x) in molten chloride (MCl_2) at different temperatures, C_{MO_x} (mol%).[31,38)]

Temperature, T /K	MgO in $MgCl_2$	CaO in $CaCl_2$
1073	0.63	13
1173	1.5	20
1273	2.1	21[a]
1373	2.9	23[a]

a: Estimated by extrapolating the reported liquidus line.

product (MO_x) in the system. Okabe *et al.*[30)] found that the calcium-halide flux deoxidation (Fig. 1(c)) could successively deoxidize Ti to an O level below that obtained by the Ca deoxidation. This is due to the fact that the activity of the deoxidized product, a_{CaO}, in the system was greatly reduced by the dissolution of CaO in $CaCl_2$. The solubility of CaO in $CaCl_2$ is 20 mol% at 1173 K (see Table 2).[31)] Based on this finding, many studies have been carried out and significant progress has been made.[32–37)] The experimental values of the deoxidation limit of Ca/CaO equilibrium ($a_{CaO} \ll 1$, in halide flux) under most conditions are less than 50 mass ppm O.[32,35)] On the contrary, the deoxidation limit of Mg/MgO equilibrium (in $MgCl_2$ flux) is not easily decreased because the activity of MgO does not decrease due to the low solubility of MgO in $MgCl_2$ which is approximately 1.5 mol% at 1173 K.[38)]

The ultimate deoxidation limit of the above-mentioned deoxidation techniques was restrained by the increasing oxide ion concentration due to the accumulation of oxide ion in the system. By using an electrochemical method (Fig. 1(d)) that employs Ti and carbon as the cathode and anode, respectively, the accumulation of oxide ion in the reaction system can be prevented. The activity of deoxidation product can be maintained at a low level during processing.[2,13,39–42)] Under certain conditions, Ti with an O level as low as 10 mass ppm O was obtained by electrochemical deoxidation[40–42)] because the a_{CaO} was further reduced by discharging oxide ion (O^{2-}) in the system by forming CO_x on the anode of the electrochemical cell. Although the deoxidation capacity of Mg and the solubility of MgO in $MgCl_2$ are low, the O content in Ti can be reduced to below 500 mass ppm O or less[13,40)] when electrolysis is used. This is attributed to the decrease in the activity of MgO to a significantly low level. However, the activity of MgO increases when a large amount of Ti scrap is processed due to the low solubility of MgO in $MgCl_2$, and the deoxidation limit of Mg/MgO sharply increases.

In spite of effective deoxidation methods using the Ca/CaO equilibrium[22–24)] and electrochemical deoxidation in $CaCl_2$, none have been employed on an industrial scale because $CaCl_2$ attached to the surfaces of Ti must be removed by leaching with aqueous solutions after deoxidation, which causes O increase and generates a large amount of waste liquid.[13)] Although the deoxidation capacity of Mg and the solubility of MgO in $MgCl_2$ is low, the O in Ti can be effectively removed as long as a method (such as electrolysis) is found to effectively reduce the activity of MgO in the system. As shown in Table 1, the theoretical O concentration in β-Ti can be reduced to 500 mass ppm O if the activity of MgO was decreased to 0.026 at 1173 K. In addition, separating $MgCl_2$ and Mg from deoxidized Ti and its alloys by evaporation without the generation of liquid waste has been well established and employed in the Kroll process.[4,43)]

As shown in Fig. 1(e), the formation of oxyhalides of some rare earth elements in molten halide fluxes can be

utilized in deoxidation from a Ti–O solid solution. As shown in Table 1, the O contents in Ti cannot be reduced to 1000 mass ppm O or below when using the equilibrium of light rare earth metals (Nd, Pr, Ce, and La) and their oxides. However, the O level can be reduced to below 100 mass ppm O by the formation of rare earth oxychlorides (MOCl; M: rare earth metals).[9] For example, using the La/LaOCl/$LaCl_3$ equilibrium at 1173 K, an oxygen partial pressure (p_{O_2}) lower than that of the La/La_2O_3 equilibrium can be achieved, and the O level in β-Ti can be theoretically reduced to 30 mass ppm O or less. The theoretical O levels in Ti reach 100 mass ppm O or less for the M/MOCl/MCl_3 equilibrium system.

Just recently, we demonstrated a deoxidation method of Ti by using Mg as deoxidant in a $MgCl_2$–YCl_3 flux. In this system, the activity of deoxidation product (O^{2-} or MgO), $a_{O^{2-}}$ or a_{MgO}, is reduced by the formation of yttrium oxychloride (YOCl) via the reaction of $O_{in\,Ti} + Mg + YCl_3 \rightarrow MgCl_2 + YOCl$.[5] The O content of Ti can be effectively reduced to below 1000 mass ppm O under the Mg/$MgCl_2$/YOCl/YCl_3 equilibrium, far lower than that determined by the Mg/MgO equilibrium. When electrolysis is conducted in the YCl_3–$MgCl_2$ system, O^{2-} can also be expelled from the system, so the Ti is deoxidized to 100 mass ppm O.[44] In addition, even if oxide ions are introduced into the system (such as adding MgO), the deoxidation limit is still very low (360 mass ppm O at 1200 K), indicating that a large volume of Ti scrap can be deoxidized in the system.

Like Y, Ho is one of the heavy rare earth metals (REMs). It is usually found in minerals such as monazite ((Ce, Y, La, Th)PO_4), comprised of approximately 65–80% La and Ce, 15–20% Nd, and 0.035–0.12% Ho.[45] Ho is currently used for lasers, magnets, nuclear reactors, gamma-ray spectrometers, and metal halide lamps.[45–47] Compared with other REMs (e.g., Y, Nd and La), Ho still lacks a unique and extensive application field.[46] This is not because of the rarity of Ho. Ho is twenty times more abundant than silver, and the world reserves of Ho are approximately 400,000 tons.[48] With an increase in the production of Nd, which is used for permanent magnets for electric vehicle motors and other electronic devices, an oversupply of Ho may occur in the future because it is a by-product of the production of Nd and other important REMs.[45,49] In addition, continued improvements in production processes of Ho may result in excess supply in the future. Ho is forecasted to remain in oversupply throughout 2019–2026, reaching a peak of 301 t holmium oxide in 2026.[50] Furthermore, the deoxidation limit of Mg/$MgCl_2$/HoOCl/$HoCl_3$ equilibrium is expected to be far lower than that of Mg/MgO equilibrium (see Table 1), and relevant studies have not been reported. Therefore, in this study, $HoCl_3$ was introduced to the $MgCl_2$ system in order to reduce the activity of MgO to reach an O level in Ti below 500 mass ppm O.

The objective of this study is to experimentally demonstrate the deoxidation ability of Mg in $MgCl_2$–$HoCl_3$ system based on the thermodynamic analysis, which will not only provide a new method for deoxidation of Ti scraps and production of Ti powders with low O concentration, but also open up a new avenue for Ho application.

Table 3 Standard Gibbs energy of formation of some compounds in M–O–Cl (M = Ho, Y, La, Mg, Ca) systems, and the standard Gibbs energy of O dissolution in β-Ti.

Compound, i	Standard Gibbs energy of formation, $\Delta G^\circ_{f,i}$ / J·mol^{-1}						$\Delta G^\circ_{f,i}$ at 1173 K / J·mol^{-1}	Refs.
Ho_2O_3 (s)	$\Delta G^\circ_{f,i}$ =	−1864000	+ T ×	272.4	1100–1500 K		−1544500	[14]
$HoCl_3$ (l)	$\Delta G^\circ_{f,i}$ =	−950100	+ T ×	191.0	1100–1300 K		−726000	[14]
HoOCl (s)	$\Delta G^\circ_{f,i}$ =	−991900	+ T ×	172.8	1100–1500 K		−789200	Estimated*
Y_2O_3 (s)	$\Delta G^\circ_{f,i}$ =	−1892000	+ T ×	278.1	1100–1500 K		−1565800	[14]
YCl_3 (l)	$\Delta G^\circ_{f,i}$ =	−941500	+ T ×	175.6	1100–1500 K		−735500	[14]
YOCl (s)	$\Delta G^\circ_{f,i}$ =	−1075000	+ T ×	219.5	1248–1375 K		−817500	[52]
La_2O_3 (s)	$\Delta G^\circ_{f,i}$ =	−1794000	+ T ×	284.8	1100–1500 K		−1459900	[14]
$LaCl_3$ (l)	$\Delta G^\circ_{f,i}$ =	−989400	+ T ×	167.0	1131–1500 K		−793500	[14]
LaOCl (s)	$\Delta G^\circ_{f,i}$ =	−1002000	+ T ×	172.8	1000–1200 K		−799300	[14]
MgO (s)	$\Delta G^\circ_{f,i}$ =	−608600	+ T ×	115.8	1100–1361 K		−473000	[14]
MgO (l)	$\Delta G^\circ_{f,i}$ =	−539900	+ T ×	94.1	1100–1361 K		−429500	[51]
$MgCl_2$ (l)	$\Delta G^\circ_{f,i}$ =	−592900	+ T ×	110.8	1100–1361 K		−462900	[14]
CaO (s)	$\Delta G^\circ_{f,i}$ =	−641500	+ T ×	109.8	1100–1500 K		−512700	[14]
$CaCl_2$ (l)	$\Delta G^\circ_{f,i}$ =	−760300	+ T ×	119.5	1100–1500 K		−620100	[14]
[O] in Ti[a]	$\Delta G^\circ_{1,Ti}$ =	−583000	+ T ×	88.5	1173–1373 K		−479200	[19]

* Estimated based on Eqs. (1) and (2) [9].
$\Delta G^\circ_{f,HoOCl} = \Delta H^\circ_{f,HoOCl,298K} + T{\cdot}\Delta gef_{LaOCl}$ (1)
$\Delta gef_{LaOCl} = (\Delta G^\circ_{f,LaOCl} - \Delta H^\circ_{f,LaOCl,298K})/T$ (2).
$\Delta H^\circ_{f,HoOCl,298K} = -1000800$ J·mol^{-1}; $\Delta H^\circ_{f,LaOCl,298K} = -1010900$ J·mol^{-1} [53].
a: 1/2 O_2 (g) = [O] in Ti (1 mass pct), Henrian 1 mass pct standard.

2. Thermodynamics of the Ho–O–Cl and Mg–O–Cl Systems

Table 3 lists the standard Gibbs energies of formation ($\Delta G^\circ_{f,i}$) of some compounds in M–O–Cl (M = Ho, Y, La, Mg, and Ca) systems used in this study.[14,15,51,52] The standard Gibbs energy of O dissolution in β-Ti ($\Delta G^\circ_{1,Ti}$) was also listed.[19] The reliability of the reported thermodynamic data for rare earth compounds is often low, especially for MOCl because of the limited research on the MOCl. The data of LaOCl used in this study was chosen from the database.[14] In this study, the $\Delta G^\circ_{f,i}$ for HoOCl was assessed based on eqs. (1) and (2)[9] because the thermodynamic data for HoOCl is not available in literature,

$$\Delta G^\circ_{f,HoOCl} = \Delta H^\circ_{f,HoOCl,298K} + T \cdot \Delta gef_{LaOCl} \quad (1)$$

$$\Delta gef_{LaOCl} = (\Delta G^\circ_{f,LaOCl} - \Delta H^\circ_{f,LaOCl,298K})/T \quad (2)$$

where $\Delta H^\circ_{f,HoOCl,298K}$ and $\Delta H^\circ_{f,LaOCl,298K}$ are the standard enthalpies of formation of HoOCl and LaOCl at 298 K, respectively;[53] Δgef_{LaOCl} is the Gibbs energy function of the formation of LaOCl, and T is the absolute temperature (K).

A logarithmic partial pressure such as $\log p_{O_2}$ or $\log p_{Cl_2}$ is used as the parameter in this study for an intuitive understanding of the absolute value of the chemical potential. In addition, $\log p_{O_2}$ is standardized as the dimensionless value relative to oxygen gas in the standard state (O_2 gas at 1 atm), and this p_{O_2} is generally called the partial pressure of oxygen (O_2 potential).

Because the calculation method of the phase diagrams as a function of chemical potential of O_2 and Cl_2 has been

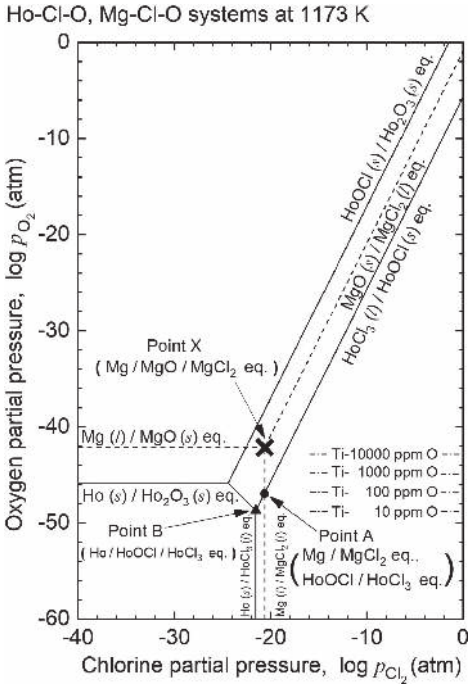

Fig. 2 p_{Cl_2}–p_{O_2} diagram of the Ho–O–Cl and Mg–O–Cl systems at 1173 K. (cf. Fig. 9)

reported in detail,[9] only a brief outline will be given here. Following the reported procedure, the superimposed isothermal p_{O_2}–p_{Cl_2} diagram of the Ho–Cl–O and Mg–Cl–O systems at 1173 K can be constructed by using the thermodynamic data listed in Table 3, as shown in Fig. 2. The p_{O_2} and O concentration in β-Ti corresponding to the equilibrium lines and points in Fig. 2 is shown in Table 1. The data for $\Delta G^\circ_{f,HoOCl}$ was assumed under the similarity with LaOCl. This will bring some error in the calculation.

Figure 2 shows that there is a stable region of HoOCl in the Ho–Cl–O system at 1173 K. Table 1 shows that the p_{O_2} determined by the Ho/HoOCl/$HoCl_3$ equilibrium (point B) is 1.9×10^{-49} atm, which is lower than that determined by the Ho/Ho_2O_3 equilibrium ($p_{O_2} = 1.4 \times 10^{-46}$ atm).

Notably, an intersection point A (the Mg/$MgCl_2$/HoOCl/$HoCl_3$ equilibrium), i.e., the intersection point between the Mg/$MgCl_2$ equilibrium line and HoOCl/$HoCl_3$ equilibrium line, is observed in Fig. 2. The p_{O_2} determined under Mg/$MgCl_2$/HoOCl/$HoCl_3$ equilibrium can be expressed using eqs. (3) through (5).

$$1/2\ O_2\ (g) + Mg\ (l) + HoCl_3\ (l) = MgCl_2\ (l) + HoOCl\ (s) \quad (3)$$

$$\Delta G^\circ_{r,(3)} = -2.303 \cdot RT \log \frac{a_{MgCl_2} \cdot a_{HoOCl}}{a_{Mg} \cdot a_{HoCl_3} \cdot {p_{O_2}}^{1/2}} \quad (4)$$

$$\Delta G^\circ_{r,(3)} = \Delta G^\circ_{f,HoOCl} + \Delta G^\circ_{f,MgCl_2} - \Delta G^\circ_{f,HoCl_3} \quad (5)$$

where a_i is the activity of substance i, R is the gas constant, and T is the absolute temperature.

The p_{O_2} at the point A can be obtained from eqs. (4) and (5) by using the data in Table 3 when a_{HoCl_3}, a_{HoOCl}, a_{Mg} and a_{MgCl_2}, are unity, as shown in Table 1.

Table 1 shows that the p_{O_2} at point A is as low as 1.4×10^{-47} atm, which is lower than that at point X ($p_{O_2} = 8.0 \times 10^{-43}$ atm).

The relationship between the p_{O_2} and the concentration of O in β-Ti ($[O]_{Ti}$ (mass% O)) can be expressed as follows,

$$1/2\ O_2\ (g) = O\ (1\ \text{mass pct, in}\ \beta\text{-Ti}), \quad (6)$$

$$\Delta G^\circ_{1,Ti} = -2.303 \cdot RT \log \frac{f_O \cdot [O]_{Ti}}{{p_{O_2}}^{1/2}} \quad (7)$$

$$= -583000 + 88.5\,T\ (J)\ [1173\text{–}1373\ K\ (900\text{–}1100^\circ C)],^{19)} \quad (8)$$

where $\Delta G^\circ_{1,Ti}$ is the standard Gibbs energy of O dissolution in β-Ti, $[O]_{Ti}$ is the O concentration in Ti expressed relative to 1 mass% O, and f_O is the Henrian activity coefficient for O dissolved in β-Ti. O dissolves in Ti obeying Henry's law, and the value of f_O is considered to be unity (standard state of O in solid Ti: 1 mass% O).

Connecting eq. (3) and eq. (6), the thermodynamic parameters for the deoxidation reaction of Ti for Mg/$MgCl_2$/$HoCl_3$/HoOCl equilibrium can be calculated using eqs. (9) through (11).

$$O\ (\text{in}\ \beta\text{-Ti}) + Mg\ (l) + HoCl_3\ (l) = MgCl_2\ (l) + HoOCl\ (s) \quad (9)$$

$$\Delta G^\circ_{\text{deox, Mg/MgCl}_2\text{/HoOCl/HoCl}_3} = -2.303 \cdot RT \log \frac{a_{MgCl_2} \cdot a_{HoOCl}}{f_O \cdot [O]_{Ti} \cdot a_{Mg} \cdot a_{HoCl_3}} \quad (10)$$

$$\Delta G^\circ_{\text{deox, Mg/MgCl}_2\text{/HoOCl/HoCl}_3} = \Delta G^\circ_{f,HoOCl} + \Delta G^\circ_{f,MgCl_2} - \Delta G^\circ_{f,HoCl_3} - \Delta G^\circ_{1,Ti} \quad (11)$$

The O concentration in β-Ti in the Mg/$MgCl_2$/$HoCl_3$/HoOCl equilibrium system can be calculated from eqs. (10) and (11) using the data in Table 3 when a_{HoCl_3}, a_{HoOCl}, a_{Mg} and a_{MgCl_2}, are unity, as shown at the end of Table 1. Pure $HoCl_3$ (l) and $MgCl_2$ (l) are considered at eq. (9), which has some deviation from the experiments in which the mixture of $HoCl_3$ and $MgCl_2$ was employed as the flux.

Table 1 shows that the O concentration in the β-Ti under the Mg/$MgCl_2$/$HoCl_3$/HoOCl equilibrium at 1173 K is approximately 80 mass ppm O, which is much lower than that of Mg/MgO equilibrium (19300 mass ppm O at 1173 K). The O level in metallic Ti, therefore, could be directly deoxidized to 1000 mass ppm O or less by Mg in $MgCl_2$–$HoCl_3$ flux through the following reactions:

$$O\ (\text{in Ti}) + Mg\ (\text{in flux}) \rightarrow MgO\ (s) \quad (12)$$

$$MgO\ (s) + HoCl_3\ (\text{in flux}) \rightarrow MgCl_2\ (\text{in flux}) + HoOCl\ (s) \quad (13)$$

The O concentration in β-Ti as a function of temperature under the Mg/$MgCl_2$/$HoCl_3$/HoOCl equilibrium is plotted by using the data calculated from eqs. (10) and (11) at different temperatures, as shown in Fig. 3. The Mg/MgO, Ho/Ho_2O_3, and Ho/HoOCl/$HoCl_3$ equilibrium (heavy lines) were also provided for a reference. As can be seen in Fig. 3, the Mg/$MgCl_2$/$HoCl_3$/HoOCl equilibrium line is much lower than the Mg/MgO line, and the O level in Ti can be reduced to approximately 100 mass ppm O by using the Mg/$MgCl_2$/$HoCl_3$/HoOCl equilibrium. Figure 3 also indicates that deoxidation limit is likely to be lower at lower temperatures when the same deoxidant is used.

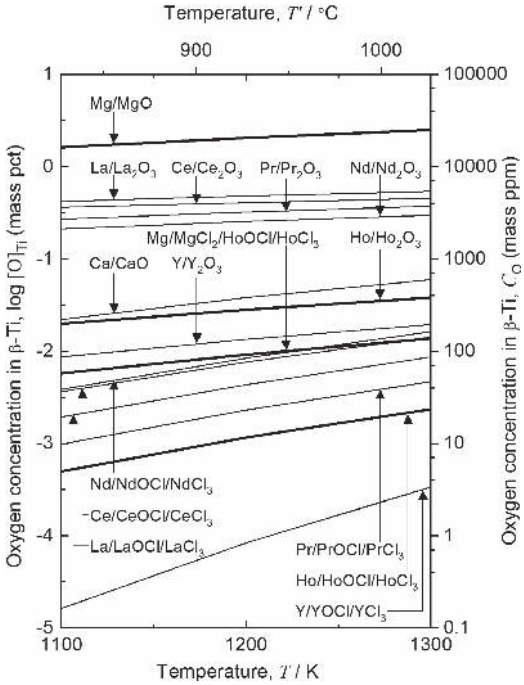

Fig. 3 Temperature dependence of O concentration in β-Ti determined by the M/M_2O_3 and $M/MOCl/MCl_3$ (M: Ho, Y, La, Ce, Pr, or Nd) equilibria; the Mg/MgO, Ca/CaO, and $Mg/MgCl_2/HoOCl/HoCl_3$ equilibria are also shown.[9,14)]

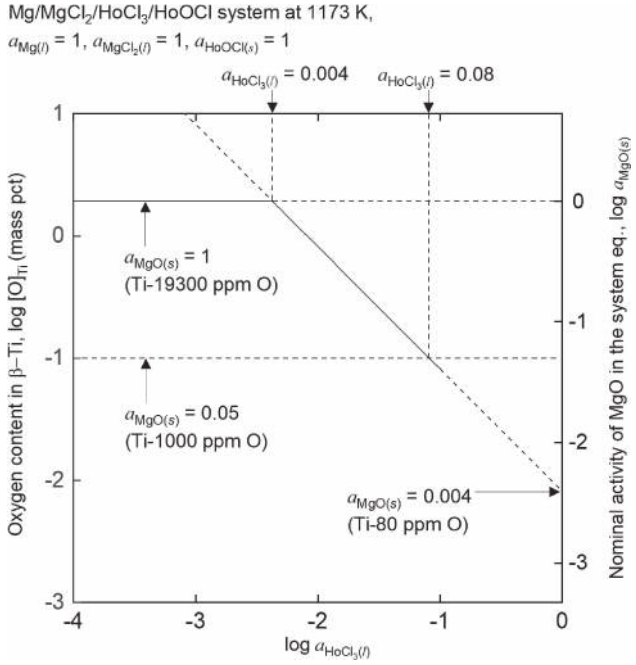

Fig. 4 Deoxidation limit of Ti in the presence of Mg, $MgCl_2$ and HoOCl *vs* the logarithm of activity of $HoCl_3$ ($a_{HoCl_3} = n_{HoCl_3}/(n_{MgCl_2} + n_{HoCl_3})$) at 1173 K. The nominal activity of MgO (a_{MgO}) in the system is also shown (cf. Fig. 8).

Equation (10) can be represented as eq. (14) when the activity of $MgCl_2$ (l), Mg (l), and HoOCl (s) are considered to be unity ($a_{MgCl_2} = 1$, $a_{Mg} = 1$, $a_{HoOCl} = 1$).

$$\log [O]_{Ti} = -\log a_{HoCl_3} + \frac{\Delta G^{\circ}{}_{deox,\,Mg/MgCl_2/HoOCl/HoCl_3}}{2.303 \cdot RT} \quad (14)$$

The diagram as a function of the O concentration in Ti and the logarithm of activity of $HoCl_3$ ($\log a_{HoCl_3}$) in the presence of Mg, $MgCl_2$, and HoOCl at 1173 K are constructed in Fig. 4 using the data calculated from eq. (14). Pure $MgCl_2$ (l), Mg (l) and HoOCl (s) are considered at eq. (14), which has some deviation from the experiments. The nominal a_{MgO} in the system is also shown in Fig. 4. Figure 4 shows that the O concentration in Ti decreased as the a_{HoCl_3} increases when Mg is present in the system as a deoxidant. This effective deoxidation is caused by the formation of HoOCl by the reaction of the deoxidized product MgO with $HoCl_3$. For example, the deoxidation limit is 19300 mass ppm O, when the a_{HoCl_3} is low (such as 0.004) and the a_{MgO} is unity. The O concentration in metallic Ti decreased to 80 mass ppm O when the a_{MgO} was decreased to 0.004 ($a_{HoCl_3} = 1$). When the a_{MgO} in the system is less than 0.05 by keeping the a_{HoCl_3} at a large value, the O concentration in metallic Ti can be reduced to less than 1000 mass ppm O.

3. Experimental

3.1 Materials

The Ti samples used in this study were two Ti wires with a diameter of 2 mm and 1.6 mm, respectively, and the corresponding O concentration in these two Ti wires was approximately 1060 and 710 mass ppm O, respectively. A Ti sample with an O concentration of 240 mass ppm O was also used.

The chemical reagents used in the experiments were anhydrous $MgCl_2$ ($\geq$ 98.00 mass pct, white powder, Sigma–Aldrich Chemical Industries, Ltd) and MgO ($\geq$ 98.00 mass pct, white powder, Wako Pure Chemical Industries, Ltd.), respectively. The metallic Ho ($\geq$ 99.00 mass pct, bulk) was provided by Santoku Co., Ltd., and Ag shot ($\geq$ 99.99 mass pct,) was provided by Ijima Kingin Kogyo Co., Ltd.

3.2 Experimental procedures

The Ti wire with a diameter of 1.6 mm was cut into a length of approximately 16 mm and bent into a U-shape (abbreviated as Ti-1.6U), while the wire with a diameter of 2.0 mm was directly cut into a length of approximately 10 mm (abbreviated as Ti-2.0L). The Ti sample with an O concentration of approximately 240 mass ppm O was cut from a bulk mass into a cube with 2–3-mm sides (abbreviated as Ti-2B). The mass of each Ti sample was approximately 0.1 g. Metallic Ho with a diameter of approximately 4–5 mm was cut from a large bulk in order to provide a lager superficial area.

The initial amounts of samples and reagents in the Ti crucible for the experiments are listed in Table 4. Figure 5 shows a schematic of the apparatus used for deoxidation experiments. First, the metals and reagents were weighed in appropriate quantities. The Ho fragment and Ag shots were placed at the bottom of a Ti crucible (25.4 mm O.D. $\times$ 0.8t $\times$ 80L). Mg forms with the following displacement reaction:

$$Ho\ (s) + 3/2\ MgCl_2\ (l) = HoCl_3\ (l) + 3/2\ Mg\ (l) \quad (15)$$

The Mg alloys with Ag and stays at the bottom of Ti crucible. The influence of Ag on the activity of the Mg

Table 4 Initial amounts of samples and reagents in the Ti crucible for the experiment at 1173 K.

Exp. No.[a]	Initial amount of samples in the titanium crucible[b], m /g (n /mol)				Fraction of $HoCl_3$
	$MgCl_2$	MgO	Ho	Ag[e]	
180507-1[c,d]	12.4	0.800	6.93	0.756	0.2
	(0.131)	(0.0200)	(0.0420)	(0.00700)	
180507-2[c]	13.1		4.12	0.454	0.2
	(0.138)		(0.0250)	(0.00420)	
180706-1[c,d]	21.7	2.82	17.3	1.89	0.2
	(0.228)	(0.0700)	(0.105)	(0.0175)	
180706-2[c]	23.1		13.4	1.46	0.4
	(0.243)		(0.0810)	(0.0135)	
180706-3[c]	22.7		18.1	1.98	0.6
	(0.238)		(0.110)	(0.0183)	
180706-4[c]	22.5		22.3	2.43	0.8
	(0.236)		(0.135)	(0.0225)	
180706-5[c]	21.4		24.7	2.70	1.0
	(0.225)		(0.150)	(0.0250)	

a: Sequence of Exp. no. is listed with an increment of fraction of $HoCl_3$ in $MgCl_2$.
b: Several Ti wires and shots (ca. 2.4 g in total) were inserted into feedstock as a monitor of p_{O_2}.
c: Ho (s) + $MgCl_2$ (l) → $HoCl_3$ (l) + Mg (l) is expected to occur.
d: MgO (s) +$HoCl_3$ (l) → HoOCl (s) + $MgCl_2$ (l) is expected to occur.
e: The nominal mole fraction of Mg in Ag-Mg alloy is 0.9.

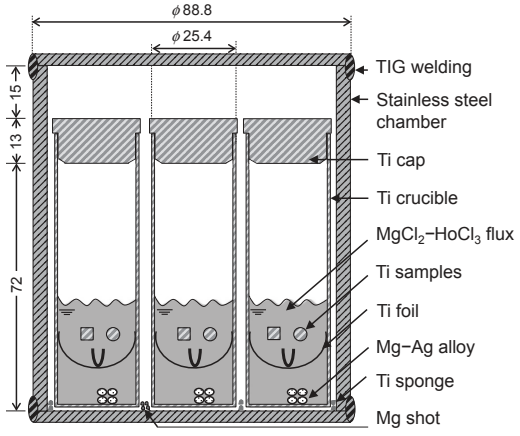

Fig. 5 Schematic of the experimental apparatus (cf. Fig. 6).

deoxidant, a_{Mg}, was considered to be small due to the small amount of Ag. The MgO powder was then set on the metals for some experiments as required. The circular Ti foils with five holes (1 mm in diameter) were placed on the metals and MgO to avoid direct physical contact of them with the Ti samples. The above-mentioned Ti samples (Ti-1.6U and Ti-2.0L, 10 each; 4 Ti-2B, ca. 2.4 g in total) were placed on the Ti foil. Then, the $MgCl_2$ powder was added into the crucible. Finally, the Ti crucible was closed with a Ti cap.

As shown in Fig. 5, the Ti crucibles were placed in a stainless-steel chamber (88.8 mm O.D. × 3 t × 100 L). The Ti sponge (approximately 6 g) was placed outside the Ti crucibles to absorb moisture, while the Mg particle (approximately 2 g) was placed outside the Ti crucibles to minimize the transport of Mg from the inside to the outside of the Ti crucible. Finally, the stainless-steel chamber was sealed using tungsten inert gas (TIG) welding.

The stainless-steel chamber was placed in a muffle furnace, and then heated to 1173 K. The holding time was 173 ks, which was estimated to be long enough to equilibrate the system based upon the known diffusion coefficient of O in β-Ti,[54] assuming a homogeneous distribution of the O dissolved in the Ti samples. This was also confirmed by the experiments in which the O concentration of Ti samples with different initial O concentrations was almost the same after the deoxidation process.[5]

After holding at 1173 K for 173 ks, the stainless-steel chamber was removed from the muffle furnace and directly quenched in water. The cap of the stainless-steel crucible was then mechanically removed.

The Ti crucibles were taken out from the chamber and then vertically bisected using the grinding wheel cutting machine. Three portions of the salts were taken from the bottom, middle, and top parts of the flux, respectively.

The Ti samples were picked out and then cleaned in sequence with acetic acid solution, diluted hydrochloric acid solution, and distilled water to remove the salts and Mg attached to the surface.

3.3 Analysis

First, the salts after thermochemical deoxidation was grinded into a fine powder with a mortar and pestle in the glove box. The phase of different parts of the salt was then determined using X-ray diffraction (XRD, Bruker, D2 Phaser, Cu-Kα radiation).

The O concentrations in the Ti samples were analyzed by the inert gas fusion technique using a TC-600 (LECO Corporation). The samples were chemically polished with $HF–HNO_3–H_2O$ (1:4:10) and then rinsed in sequence with distilled water, alcohol, and acetone before drying. The chemical etching is only for removing the oxide layer on the surface of Ti sample, which forms after deoxidation process, the residual salts, and deoxidation products (HoOCl) attached to the surface of Ti sample. In the analysis, the sample was melted in a graphite crucible under the inert gas, and the evolved gases were measured using infrared absorption. Ti samples were melted with approximately 1 g of high-purity nickel (Ni flux 502-344, 4 ± 2 μg O, LECO Corporation) in order to smoothly extract the O. A standard Ti sample (Ti pin 502-879, 930 ± 80 mass ppm O, LECO Corporation) was used for calibration in the O analysis. Another standard Ti sample (Ti pin 502-881, 500 ± 50 mass ppm O) was used for cross-checking of the accuracy of the measured values. The error in the analysis of O concentration in the Ti samples was due to the uncertainty of the calibration curve and the fluctuation in the measured total amount of O in the Ni flux. The analytical error for the calibration using the Ti standard samples was within 9%. The fluctuation in measured O content in the l-g Ni flux was approximately 2 μg O, and those for the other blank values were negligibly small.

4. Results and Discussion

Table 4 shows the initial amounts of samples and reagents in the Ti crucible for the experiment. Based on the initial feedstock listed in Table 4 and the stoichiometric coefficient for the displacement reaction shown in eq. (15), the complete disappearance of metallic Ho was expected in this study. Figure 6 shows a schematic and a photograph of the sectioned Ti crucible used in Exps. #180507-1 to #180706-5, which shows that the Ti samples (Ti-1.6U, Ti-2.0L, and Ti-2B) were totally immersed in the flux in the deoxidation process.

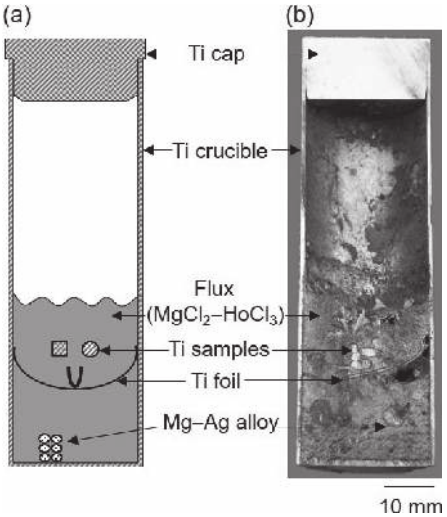

Fig. 6 (a) Schematic and (b) photograph of the Ti crucible used in the experiments (cf. Fig. 5).

Table 5 Experimental conditions and the O concentration of the Ti samples before and after the experiment.

Exp. No.[a]	Experimental Conditions	Types of Ti samples	O concentration, C_O (mass ppm O)[c]		Maximum analysis error of O concentration after exp. (%)
			Initial[b]	After Exp.[c]	
180507-1[d]	1173 K / 173 ks	Ti-1.6U	710	1680, 1690, 1790	7
		Ti-2.0L	1060	1360, 1650, (1670)	7
180507-2	1173 K / 173 ks	Ti-1.6U	710	1640, 1690	7
		Ti-2.0L	1060	1640, 1630	7
180706-1[d]	1173 K / 173 ks	Ti-2B	240	(2120), (2190)	10
		Ti-1.6U	710	(2070), (2120), (2230)	10
		Ti-2.0L	1060	(2140), (2180)	10
180706-2	1173 K / 173 ks	Ti-2B	240	710, 770, 900	12
		Ti-1.6U	710	690, 730, 730	12
		Ti-2.0L	1060	890, 900, 980	11
180706-3	1173 K / 173 ks	Ti-2B	240	810, 810	12
		Ti-1.6U	710	840, 840	12
		Ti-2.0L	1060	800, 830	12
180706-4	1173 K / 173 ks	Ti-2B	240	520, 590	13
		Ti-1.6U	710	520, 540	13
		Ti-2.0L	1060	530, 640	13
180706-5	1173 K / 173 ks	Ti-2B	240	370, 380	15
		Ti-1.6U	710	370, 390	15
		Ti-2.0L	1060	370, 390	14

a: Initial amounts of samples for equilibrium experiments are shown in Table 4, and the sequence of Exp. Nos. is listed with increasing fraction of $HoCl_3$ in $MgCl_2$.
b: Average value is given.
c: Value in a parenthesis includes a lot of uncertainty (out of the calibration line).
d: MgO added to the initial feedstock.
e: Representative analytical conditions:
Standard sample: Ti pin ~0.1 g, 500 ± 50 mass ppm O, part number: 502-881
Standard sample: Ti pin ~0.1 g, 930 ± 80 mass ppm O, part number: 502-879
Ni flux: ~1.0 g, 4 ± 2 μg O, part number: 502-344.

The experimental conditions and the O concentrations of the Ti samples before and after thermochemical deoxidation in molten $MgCl_2$–$HoCl_3$ at 1173 K are summarized in Table 5. Most of the Ti samples in each experiment reached the same O concentration despite different initial O concentrations. This indicates that the reaction time of 173 ks was sufficient for the diffusion of O dissolved in Ti.

Table 5 also clearly indicates that direct deoxidation of Ti by Mg in molten $MgCl_2$–$HoCl_3$ is effective. The O content in Ti was reduced down to range from 560 to 1650 mass ppm O (Exps. #180507-2, #180706-2, #180706-3, and #180706-4). Under some conditions, the O concentrations of the Ti-wires were lowered to below 500 mass ppm O (Exp. #180706-5). These values are much lower than 12100 mass ppm O that was obtained by the Mg/MgO equilibrium.[5] This can be explained as follows: The $HoCl_3$ was first produced in the system by the reaction shown in eq. (15). The Ti samples were then mixed with Mg and $MgCl_2$–$HoCl_3$ flux (or $HoCl_3$ flux) (Table 4). The deoxidation of Ti by Mg occurs according to the reactions shown in eq. (12) and eq. (13). Therefore, the activity of the deoxidized product a_{MgO} could be reduced by $HoCl_3$ to a low level, while that in Mg/MgO equilibrium is unity.

In addition, the O concentration in the Ti decreased with the increasing concentration of $HoCl_3$. In Exp. #180706-5, where the concentration of $MgCl_2$ is, in principle, almost zero via the displacement reaction shown in eq. (15), the O content in the Ti samples with an initial O concentration of 1060 mass ppm O was reduced to 380 mass ppm O. Except for the recent report by Zheng *et al.* of the deoxidation of Ti by Mg in $MgCl_2$–YCl_3 system[5] and by Zhang *et al.* of the reduction of TiO_2 by using the hydrogen-assisted magnesiothermic reduction,[55] there have been no reports about the reduction of O in Ti to lower than 1000 mass ppm O using Mg as a deoxidant without using an electrochemical method.

MgO was added into the initial feedstock to compare the effect of an increased activity of MgO on the O concentration in the Ti samples in Exps. #180507-1 and #180706-1 (see Table 4). Table 5 shows that the O concentrations in the Ti samples of Exp. #180507-1 are almost the same as those of Exp. #180507-2, in which no MgO was added. The O concentration in the Ti samples of Exp. #180706-1, in which a large amount of MgO was added, is the highest among all the experiments carried out in this study. However, the O concentration in the Ti samples of Exp. #180706-1 (2150 mass ppm O) are still much lower than that of Mg/MgO equilibrium (12100 mass ppm O). These results indicate that the formation of HoOCl substantially decreased the a_{MgO} in the system, and the deoxidation of Ti by Mg in the $MgCl_2$–$HoCl_3$ system is feasible and effective even when processing large amounts of Ti scrap.

Figure 7 shows the XRD patterns of the flux after deoxidation in Exp. #180706-1 (initial amounts of reagents are shown in Table 4). As can be seen in Fig. 7, peaks of HoOCl,[56,57] $HoCl_3$,[58] and $MgCl_2$[59] were detected, which affirms that the reactions shown in eq. (15) and eq. (16) were occurred when the metallic Ho was mixed with $MgCl_2$ and MgO,

$$\Delta G^{\circ}_{r,(15)} = -31.6\,\text{kJ at } 1173\,\text{K}.^{14)}$$
$$\text{MgO}\ (s) + \text{HoCl}_3\ (l) = \text{MgCl}_2\ (l) + \text{HoOCl}\ (s) \qquad (16)$$
$$\Delta G^{\circ}_{r,(16)} = -53.1\,\text{kJ at } 1173\,\text{K}.^{14)}$$

In addition, Fig. 7 shows that ($MgCl_2$ (l) + $HoCl_3$ (l)) mainly appeared in the top of the flux, while HoOCl (s) is found at the middle and bottom of the flux. This result indicates that the two phases are stable and separated from each other after the system reached equilibrium. Because HoOCl deposited at the bottom of container after deoxidation, HoOCl can be easily transferred to the recovery process, and carbo-chlorination (HoOCl (s) + Cl_2 (g) + C $(s) \rightarrow$ $HoCl_3$ (s, l) + CO_x (g)) is one of the candidate techniques.[60]

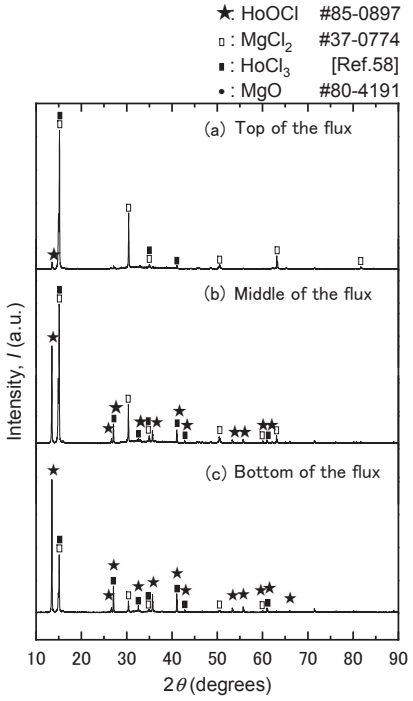

Fig. 7 XRD patterns of the flux after the deoxidation process of Exp. 180706-1. XRD peaks of HoOCl,[56,57] $HoCl_3$,[58] $MgCl_2$,[59] and MgO are shown with the filled star, filled square, hollow square, and filled circle, respectively. There was no peak matching MgO. The initial amounts of the reagents are shown in Table 4.

Furthermore, from the O concentration of the Ti samples in Exps. #180507-1 to #180706-4, the deoxidation limit of Ti in the $Mg/MgCl_2/HoCl_3/HoOCl$ equilibrium system is considered to be 560–2150 mass ppm O when a_{Mg} and a_{HoOCl} were close to unity. The a_{MgO} value was significantly reduced by the formation of HoOCl in the $MgCl_2$–$HoCl_3$ system. Therefore, O content in Ti can be directly reduced to less than 1000 mass ppm O by Mg in the $MgCl_2$–$HoCl_3$ system.

Figure 8 shows the dependence of the O concentrations of Ti samples on the a_{HoCl_3} at 1173 K in the presence of Mg, $MgCl_2$, and HoOCl. The experimental a_{HoCl_3} was determined using mole fraction of $HoCl_3$, i.e., $x_{HoCl_3} = n_{HoCl_3}/(n_{MgCl_2} + n_{HoCl_3})$ from the values of the initial feedstock assuming that the activity coefficients of $HoCl_3$ in $MgCl_2$ were unity. The calculated O concentrations in Ti are also plotted in Fig. 8 (cf. Fig. 4). Figure 8 shows that the O concentrations under most conditions are smaller than 1000 mass ppm O, which indicates that the deoxidation in this system is effective. Both experimental and theoretical results indicate that the O concentrations of Ti samples decreased with the increasing a_{HoCl_3}. In addition, a deviation between the experimental results and the calculated data was also observed. One of the sources of the deviation can be the error of $\Delta G^{o}_{f,HoOCl}$. For example, if $\Delta G^{o}_{f,HoOCl}$ is +19 kJ/mol larger than the estimated data, the calculated deoxidation limit of Ti ($a_{Mg} = 1$, $a_{MgCl_2} = 1$, $a_{HoOCl} = 1$, $a_{HoCl_3} = 1$) increases by approximately 500 mass ppm O.

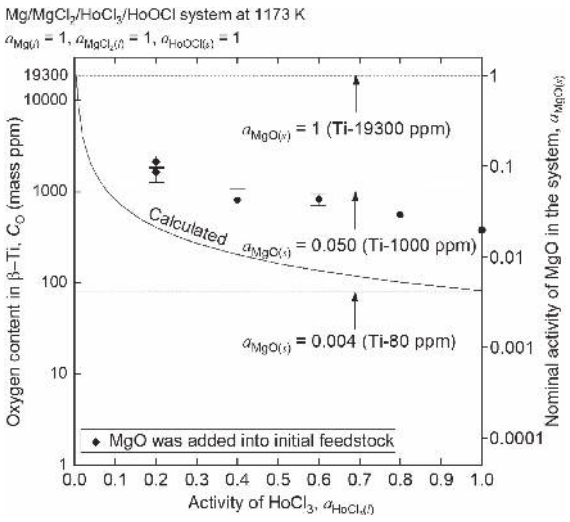

Fig. 8 Experimentally determined O concentration in the Ti samples *vs* $HoCl_3$ activity (a_{HoCl_3}); the calculated deoxidation limit of Ti is also plotted in the figure (cf. Fig. 4). The experimental a_{HoCl_3} values were calculated using $n_{HoCl_3}/(n_{MgCl_2} + n_{HoCl_3})$.

5. Feasibility of Deoxidation by Using an Electrochemical Method

To decrease the O concentration in Ti, electrochemical deoxidation that employs carbon and Ti as the anode and cathode, respectively, may be effective. Aside from the formation of HoOCl, the residual O^{2-} can be discharged out from the system in the form of CO_x when electrolysis is conducted in the $MgCl_2$–$HoCl_3$ system. The a_{MgO}, therefore, could be further reduced, making the deoxidation of Ti scrap more effective.

Figure 9 shows the E–pO^{2-} diagram of the M–O–Cl system (M = Ho, Mg) plotted using the thermodynamic data listed in Table 3. The detailed calculation method is available in literatures.[44,61]

The vertical axis in the diagram represents the oxidation–reduction potential, E (V). The reference potential is defined by the Cl_2 (g)/Cl^- ($p_{Cl_2} = 1$) equilibrium, i.e., the standard Gibbs energy of formation of the chloride ion ($\Delta G^{\circ}_{f,Cl^-}$) is 0, which is expressed as follows,

$$1/2\ Cl_2\ (g) + e^- = Cl^-\ (\text{in flux}) \qquad (17)$$

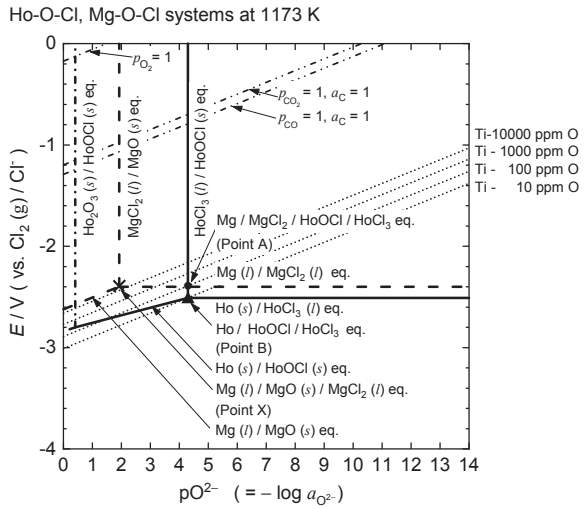

Fig. 9 E–pO^{2-} diagram of the M–O–Cl system (M = Ho, Mg) at 1173 K ($\Delta G^{\circ}_{f,O^{2-}} = 33$ kJ). (cf. Fig. 2).

$$\Delta G^{\circ}_{f,Cl^-} \equiv 0 \text{ (or } E^{\circ}_{Cl_2/Cl^-} \equiv 0) \quad (18)$$

The horizontal axis represents the pO^{2-}, and is defined using the activity of the oxide ion in the flux ($a_{O^{2-}}$) as follows.

$$pO^{2-} \equiv -\log a_{O^{2-}} \quad (19)$$

$a_{O^{2-}}$ and the activity of chloride ion in the flux, a_{Cl^-}, were determined by using the anion mole fraction of oxide ion, $x_{O^{2-}}$, and the anion mole fraction of chloride ion, x_{Cl^-}, respectively. ($x_{O^{2-}} = n_{O^{2-}}/(n_{O^{2-}} + n_{Cl^-})$, n_i: mole amount of anion i in the system). Because the solubility of oxide ions in the chloride flux is usually low, a chloride flux ($MgCl_2$) was employed as the solvent in the high pO^{2-} region. The approximation, i.e., $a_{Cl^-} \approx 1$ (or, $pCl^- \approx 0$, at high pO^{2-} region), therefore, was employed in this study. In addition, the standard state for O^{2-} in this study was defined assuming that the activity of O^{2-} is unity when $x_{O^{2-}} = 1$ (i.e., $a_{O^{2-}} \equiv 1$ at $x_{O^{2-}} = 1$).

The standard Gibbs energy of formation of oxide ion ($\Delta G^{\circ}_{f,O^{2-}}$) is essential in calculation of the E–pO^{2-} diagram, which is defined according to the method of Littlewood:

$$\Delta G^{\circ}_{f,O^{2-}} = \Delta G^{\circ}_{f,MgO\ (l)} + 2\ \Delta G^{\circ}_{f,Cl^-} - \Delta G^{\circ}_{f,MgCl_2\ (l)} \quad (20)$$

Connecting eqs. (18) and (20), eqs. (21) and (22) can be derived as follows.

$$1/2\ O_2\ (g) + 2\ e^- = O^{2-} \text{ (in flux)}, \quad (21)$$

$$\Delta G^{\circ}_{f,O^{2-}} = \Delta G^{\circ}_{f,MgO\ (l)} - \Delta G^{\circ}_{f,MgCl_2\ (l)} = 33.4\,\text{kJ at } 1173\,\text{K}^{14,51)} \quad (22)$$

Point A in Fig. 9 corresponds to point A in Fig. 2 and point B in Fig. 9 corresponds to point B in Fig. 2. The same O concentration (10–10000 mass ppm O) in Ti (dash lines) are also plotted in Fig. 9 using eqs. (6) and (21). When the $a_{O^{2-}}$ in $MgCl_2$ decreases (i.e. the pO^{2-} of the system increases), the O concentration in Ti decreases in equilibrium with $Mg/MgCl_2$.

Figure 9 indicates that metallic Mg is deposited on the cathode and works as a deoxidant when electrolysis is conducted in a $MgCl_2$–$HoCl_3$ flux. The Mg deoxidant removes the O dissolved in Ti (cathode) as O^{2-}, and forms HoOCl. By the formation of HoOCl, pO^{2-} increases to more than 4.0 (i.e., $a_{O^{2-}}$ significantly decreases). The concentration of O^{2-} further decreases due to the electrochemical oxidation of O^{2-} on the carbon anode to form CO_x gas. The above-mentioned electrochemical methods indicate that the electrochemical deoxidation of Ti scraps in $MgCl_2$–$HoCl_3$ system will be more effective.

The deoxidation process proposed in this study could be useful not only for the refining process of Ti scrap but also for direct O removal from primary Ti and its powder in Ti production process from TiO_2, as shown in Fig. 10. The O content of Ti powder obtained from direct reduction of TiO_2 by metal is usually high. By adopting this new deoxidation process to produce low O Ti powders by utilizing Mg as deoxidizer and rare earth oxyhalide as reaction booster (O^{2-} activity reducer), the O content in Ti can be reduced to below 1000 mass ppm O. After deoxidation, the Mg and $MgCl_2$ attached to the deoxidized Ti materials are removed and recovered by vacuum distillation without the generation of liquid waste, which is particularly advantageous for Ti powders which have large specific areas. In addition, $MgCl_2$ is available as a by-product of Ti sponge production. Furthermore, HoOCl generated during the proposed process can be easily recovered by carbo-chlorination, which will be conducted in our future study. Currently, the process for directly deoxidizing Ti powders is not employed on an industrial scale. The authors believe that the deoxidation process illustrated in Fig. 10 has the potential to be used in industrial applications.

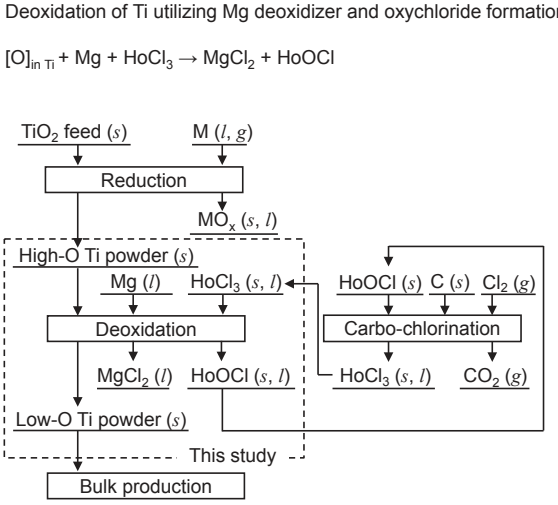

Fig. 10 New deoxidation process for producing Ti powders by utilizing Mg as deoxidizer and rare earth element as reaction booster (O^{2-} activity reducer).

6. Conclusions

The thermochemical deoxidation of Ti *via* the reaction O (in Ti) + Mg + $HoCl_3$ → HoOCl + $MgCl_2$ was conducted at 1173 K. The experimental results indicate that O concentration in Ti can be reduced to 1000 mass ppm O or less. These results and E–pO^{2-} diagram indicate that electrochemical deoxidation in the $MgCl_2$–$HoCl_3$ flux has the potential to be used for the deoxidation of Ti scrap and thus become an application of Ho metal.

Acknowledgments

The authors are grateful to Mr. Chenyi Zheng, Mr. Akihiro Iizuka, and Mr. Takara Tanaka at The University of Tokyo for their helpful suggestions and help in the experiment. This work was financially supported by the Japan Society for the Promotion of Science (JSPS) through a Grant-in-Aid for Scientific Research (S) (KAKENHI Grant No. 26220910, and KAKENHI Grant No. 19H05623). One of the authors (L.X. Kong), who is an associate professor in Faculty of Metallurgcial and Energy Engineering, Kunming Universtiy of Science and Technology, and a postdoctoral research fellow in Institute of Industrial Science, The University of Tokyo, would like to thank the China Scholarship Council (CSC No. 201708530005), and the High-level Talent Platform Construction Program of Kunming University of Science and Technology (Grant No. KKKP201752023) for providing financial support during this research.

REFERENCES

1) D.R. Lide: *CRC Hand Book of Chemistry and Physics*, 85th ed., (CRC Press, Boca Raton, FL, 2005).
2) G.Z. Chen, D.J. Fray and T.W. Farthing: Metall. Mater. Trans. B **32** (2001) 1041–1052.
3) L.G. Woodruff, G.M. Bedinger and N.M. Piatak: *Titanium, Chapter T, Critical Mineral Resources of the United States—Economic and Environmental Geology and Prospects for Future Supply*, ed. by K.J. Schulz, J.H. DeYoung, Jr., R.R. Seal II, and D.C. Bradley, (U.S. Geological Survey Professional Paper 1802, 2017) pp. T1–T23.
4) W. Kroll: Trans. Electrochem. Soc. **78** (1940) 35–47.
5) C.Y. Zheng, T. Ouchi, A. Iizuka, Y. Taninouchi and T.H. Okabe: Metall. Mater. Trans. B **50** (2019) 622–631.
6) R.W. Evans, R.J. Hull and B. Wilshire: J. Mater. Process. Technol. **56** (1996) 492–501.
7) T. Suzuki: Titanium Japan **57** (2009) 21–29 (in Japanese).
8) Y. Taninouchi, Y. Hamanaka and T.H. Okabe: Proceedings of Ti-2015: The 13th World Conference on Titanium, (August 16–20, 2015, San Diego, USA, 2015) pp. 165–170.
9) T.H. Okabe, C.Y. Zheng and Y. Taninouchi: Metall. Mater. Trans. B **49** (2018) 1056–1066.
10) Y. Waseda and M. Isshiki (ed.): *Purification Process and Characterization of Ultra High Purity Metals*, (Springer-Verlag Berlin Heidelberg, Berlin, Germany, 2001) pp. 3–37.
11) T.H. Okabe and Y. Umetsu: Proceedings of Titanium'99: Science and Technology, (1999) pp. 1417–1424.
12) K.A. Gschneidner, Jr.: J. Alloy. Compd. **193** (1993) 1–6.
13) Y. Taninouchi, Y. Hamanaka and T.H. Okabe: Metall. Mater. Trans. B **47** (2016) 3394–3404.
14) I. Barin: *Thermochemical Data of Pure Substance*, 3rd ed., (Wiley-VCH, Weinheim, Germany, 1995).
15) T.H. Okabe, Y. Taninouchi and C.Y. Zheng: Metall. Mater. Trans. B **49** (2018) 3107–3117.
16) O. Kubaschewski and W.A. Dench: J. Inst. Met. **82** (1953) 87–91.
17) K. Ono and S. Miyazaki: J. Japan Inst. Metals **49** (1985) 871–875 (in Japanese).
18) R.L. Fisher: Deoxidation of Titanium and Similar Metals Using a Deoxidant in a Molten Metal Carrier, US Patent, No. 4923531A, 1990, (UK Patent No. GB 2224749A, 1989).
19) T.H. Okabe, R.O. Suzuki, T. Oishi and K. Ono: Mater. Trans., JIM **32** (1991) 485–488.
20) R.L. Fisher: Deoxidation of a Refractory Metal, US Patent, No. 5022935, (1991).
21) K. Kamihira, R. Hasegawa and O. Ogawa: Mater. Trans., JIM **34** (1993) 243–247.
22) R.L. Fisher and S.R. Seagle: Removal of Oxide Layers from Titanium Castings Using an Alkaline Earth Deoxidizing Agent, US Patent, No. 5211775 A, (1993).
23) R.L. Fisher and S.R. Seagle: *DOSS, An Industrial Process for Removing Oxygen from Titanium Turnings Scrap, Proceedings Titanium'92*, Science and Technology, vol. 3, ed. by F.H. Froes and I. Caplan, (TMS, Warrendale, PA, U.S.A., 1993) pp. 2265–2272.
24) J.-M. Oh, B.-K. Lee, C.-Y. Suh, S.-W. Cho and J.-W. Lim: Powder Metall. **55** (2012) 402–404.
25) J.-M. Oh, K.-M. Roh, B.-K. Lee, C.-Y. Suh, W. Kim, H. Kwon and J.-W. Lim: J. Alloy. Compd. **593** (2014) 61–66.
26) J.-M. Oh, H. Kwon, W. Kim and J.-W. Lim: Thin Solid Films **551** (2014) 98–101.
27) J.M. Oh, I.H. Choi, C.Y. Suh, H. Kwon, J.W. Lim and K.M. Roh: Met. Mater. Int. **22** (2016) 488–492.
28) S.-J. Kim, J.-M. Oh and J.-W. Lim: Met. Mater. Int. **22** (2016) 658–662.
29) Y. Zhang, Z.Z. Fang, Y. Xia, Z. Huang, H. Lefler, T. Zhang, P. Sun, M.L. Free and J. Guo: Chem. Eng. J. **286** (2016) 517–527.
30) T.H. Okabe, R.O. Suzuki, T. Oishi and K. Ono: Tetsu-to-Hagané **77** (1991) 93–99 (in Japanese).
31) D.A. Wenz, I. Johnson and R.D. Wolson: J. Chem. Eng. Data **14** (1969) 250–252.
32) T.H. Okabe, T. Oishi and K. Ono: J. Alloy. Compd. **184** (1992) 43–56.
33) T.H. Okabe, T. Oishi and K. Ono: Metall. Mater. Trans. B **23** (1992) 583–590.
34) T.H. Okabe, K. Hirota, Y. Waseda and K.T. Jacob: Shigen-to-Sozai **114** (1998) 813–818.
35) T.H. Okabe, K. Hirota, E. Kasai, F. Saito, Y. Waseda and K.T. Jacob: J. Alloy. Compd. **279** (1998) 184–191.
36) S.-M. Han, Y.-S. Lee, J.-H. Park, G.-S. Choi and D.-J. Min: Mater. Trans. **50** (2009) 215–218.
37) Y. Xia, Z.Z. Fang, P. Sun, Y. Zhang, T. Zhang and M. Free: J. Mater. Sci. **52** (2017) 4120–4128.
38) M. Ito and K. Morita: Mater. Trans. **45** (2004) 2712–2718.
39) T.H. Okabe, M. Nakamura, T. Oishi and K. Ono: Metall. Mater. Trans. B **24** (1993) 449–455.
40) M. Nakamura, T.H. Okabe, T. Oishi and K. Ono: Electrochemical Deoxidation of Titanium, Proceedings of International Symposium on Molten Salt Chemistry and Technology, (1993) pp. 529–540.
41) T.H. Okabe, T.N. Deura, T. Oishi, K. Ono and D.R. Sadoway: J. Alloy. Compd. **237** (1996) 150–154.
42) K. Hirota, T.H. Okabe, F. Saito, Y. Waseda and K.T. Jacob: J. Alloy. Compd. **282** (1999) 101–108.
43) K. Nakamura, T. Iida, N. Nakamura and T. Araike: Mater. Trans. **58** (2017) 319–321.
44) C.Y. Zheng, T. Ouchi, L.X. Kong, Y. Taninouchi and T.H. Okabe: Metall. Mater. Trans. B, in print (2019).
45) N. Krishnamurthy and C.K. Gupta: *Extractive Metallurgy of Rare Earths*, 2nd ed., (CRC Press, Taylor & Francis Group, Boca Raton, 2016).
46) Y. Gu: Rare Earth Information **11** (2005) 29–30 (in Chinese).
47) N. Haque, A. Hughes, S. Lim and C. Vernon: Resources **3** (2014) 614–635.
48) J. Emsley: *Nature's Building Blocks: An A–Z Guide to the Elements*, (Oxford University Press, US, 2001).
49) F. Habashi: Can. Metall. Quart. **52** (2013) 224–233.
50) *Rare Earths: Global Industry, Markets and Outlook to 2026*, 16th ed., (Roskill Information Services, London, UK, 2016).
51) M.W. Chase: *NIST-JANAF Thermochemical Tables*, 4th ed., (American Institute of Physics, 1998).
52) Y.B. Patrikeev, G.I. Novikov and V.V. Badovskii: Russ. J. Phys. Chem. **47** (1973) 284.
53) D.D. Wagman, W.H. Evans, V.B. Parker, R.H. Schumm, I. Halow, S.M. Bailey, K.L. Churney and R.L. Nuttall: J. Phys. Chem. Ref. Data **11** suppl. 2 (1982).
54) C.J. Rosa: Metall. Trans. **1** (1970) 2517–2522.
55) Y. Zhang, Z.Z. Fang, Y. Xia, P. Sun, B.V. Devener, M. Free, H. Lefler and S.L. Zheng: Chem. Eng. J. **308** (2017) 299–310.
56) D.H. Templeton and C.H. Dauben: J. Am. Chem. Soc. **75** (1953) 6069–6070.
57) K. Song and S.M. Kauzlarich: Chem. Mater. **6** (1994) 386–394.
58) V.H.P. Beck and E. Gladrow: Z. Anorg. Allg. Chem. **502** (1983) 178–184.
59) A. Ferrari, A. Braibanti and G. Bigliardi: Acta Crystallogr. **16** (1963) 846–847.
60) J.P. Gaviría and A.E. Bohé: Thermochim. Acta **509** (2010) 100–110.
61) R. Littlewood: J. Electrochem. Soc. **109** (1962) 525–534.